WIDEBAND MILLIMETER-WAVE CAVITY-BACKED BOWTIE ANTENNA

S.-W. Qu[1, *] and K. B. Ng[2]

[1]School of Electronic Engineering, University of Electronic Science and Technology of China (UESTC), Chengdu 611731, China

[2]Department of Electronic Engineering, City University of Hong Kong, Kowloon, Hong Kong, China

Abstract—Although many directive antennas operating in a narrow band of millimeter (mm) waves were reported, e.g., antennas for 60-GHz wireless local area network (WLAN), their wideband counterparts are still unpopular. Cavity-backed antennas (CBAs) are widely developed and reported in microwave frequency bands, but handful of literatures can be found about mm-wave CBAs in spite that their many properties are quite suitable for mm-wave applications. This paper presents a wideband unidirectional CBA with a bowtie exciter, operating in a frequency band of $40 \sim$ over $75\,\text{GHz}$, and it is carefully analyzed in terms of influences of all components on the radiation patterns, broadside gains, and reflection coefficients of the proposed antenna. Then, the antenna prototype is built by generic printed circuit board (PCB) technologies, and measurements prove the validity of simulations.

1. INTRODUCTION

Development of millimeter (mm) wave systems has led to many innovative techniques with successful demonstrations in different potential applications, due to many advantages, e.g., large absolute operating frequency band, high data capability, confidentiality. Among these applications, the frequency band around $26\,\text{GHz}$ makes the point-to-point short-range communications possible [1], and the unlicensed bands around $60\,\text{GHz}$ provides opportunities for high-speed wireless local area networks (WLAN) [2]. The abundant spectrum resources in mm-wave frequency bands also support other applications, e.g.,

77 GHz automotive anti-collision radar [3] and 94 GHz imagers or radiometers [4].

In these systems, high-performance antennas are one of the critical components, and many kinds of mm-wave antennas have been reported, e.g., microstrip patches, horns [5, 6], slot arrays [7, 8], dielectric antennas [9, 10], printed dipoles [11–14]. They are generally designed based on integrated circuits (ICs) [15–17], low-temperature cofired ceramic (LTCC) [18], micro-machined [7, 19, 20] or commonly used substrate technologies [5, 8, 11, 14, 21–23]. The former two types infuse innovations into the mm-wave antenna technologies, but the latter are still the most popular ways so far for the majority of manufacturers and users due to their low investments on research and development.

Otherwise, from the bandwidth point of view, the currently reported antennas generally show small bandwidth for directive radiations. For instance, small bandwidth of high-order mode dielectric [9, 10] and microstrip patch antennas [23, 24] can constrainedly meet the lowest requirements of the 60-GHz WLAN. Although there are also wideband operations reported, they are limited by either the bulky dimensions [12, 25, 26] or omni-directional radiation patterns [27].

In microwave frequency bands, cavity-backed antennas (CBAs) are one of the most attractive candidates for directive wideband/ultra-wideband (UWB) applications. Although they were proposed several decades ago, their developments for modern communication systems in the past two decades are not as popular as before the 1980's [28]. Until around 2000, several works were continued by a few research groups around the world [29–34]. Li et al. reported their development on short backfire antennas (they can be considered as a specific kind of CBA) [29, 30]. Ou Yang et al. published their developed a low-profile unidirectional cavity-backed log-periodic slot antenna operating in a frequency band of 3–18 GHz [31]. One of the authors did a lot of further works on the wideband CBAs with improved radiation patterns and enhanced operating bandwidth in the State Key Lab of Millimeter Waves, City University of Hong Kong (CityU) [33]. Many inherent characteristics, e.g., their electrically large size, generally $1 \sim 2$ wavelength in total, becomes one of the superiorities at mm-wave frequencies. Moreover, their properties of high gain, large operating bandwidth, low side lobes and back lobes are also expected for many mm-wave applications. Unfortunately, researches on mm-wave CBAs are scarce so far. In [35], a cavity-backed folded dipole superstrate antenna was reported for 60 GHz applications, but the bandwidth is only 9 GHz, corresponding to a fractional bandwidth of 15%.

In this paper, an attempt to scale the previously reported CBAs for mm-wave applications were performed based on the low-cost PCB technology. The newly developed mm-wave CBA is deliberately designed to be electrically large for ease of fabrication and wideband operations, covering a large frequency band from 40 to over 75 GHz, but it is easy to shrink the bandwidth for the narrow-band applications, e.g., 60-GHz WLAN, by changing the antenna impedance matching. In this research, effects of each component necessary to build the prototype, e.g., connector and screws, on antenna performances are carefully analyzed. An antenna prototype was designed and measured, and acceptable agreements between simulated and measured standing-wave ratios (SWRs) can be observed, and discrepancies on radiation patterns are also discussed.

2. GEOMETRY

Figure 1 shows geometries of the proposed mm-wave CBA, a three-layered structure excited by a bowtie exciter. In the model, all
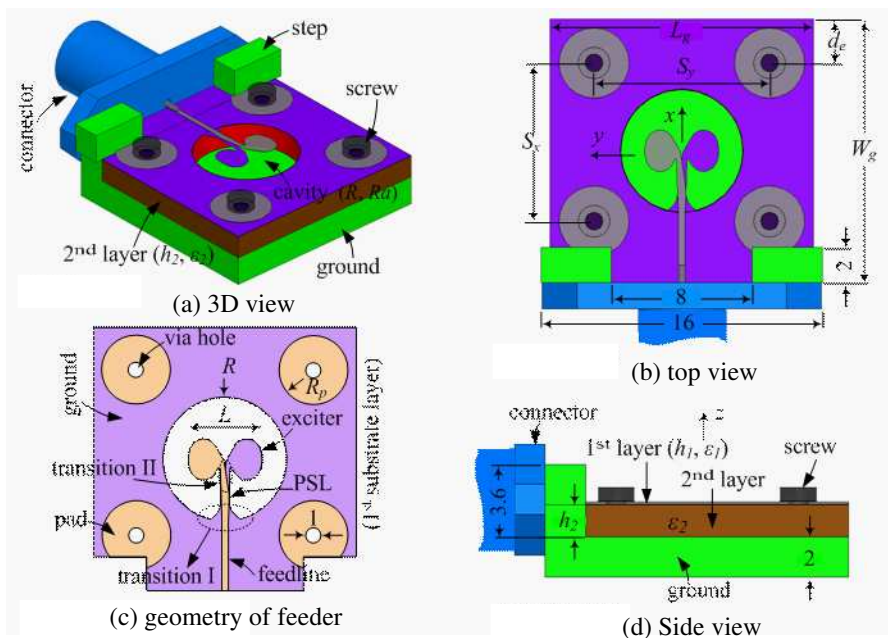

Figure 1. Geometry of the proposed mm-wave CBA with a bowtie exciter. (a) 3D view of full antenna model. (b) Top view of full antenna model. (c) Geometry of the bowtie exciter on substrate. (d) Side view of full antenna model.

components with any possible influences on antenna performances are taken into consideration in simulations, including double substrate layers, four screws to mount the substrates, real thicknesses of both substrates and cladding copper layers, four pads under the screws, a full-sized V-band connector, and two steps to mount the connector. The antenna cavity is built on a substrate layer to verify one of our design goals of integrating the CBA into the mm-wave systems based on substrate. To support the substrates and the connector, a ground with a thickness 2 mm is employed, and the selected thickness can be mechanically strong enough for experiments. Meanwhile, the substrates are mounted on the ground plane by using four screws with a diameter 1 mm, the smallest available in our lab, to decrease the influences on the radiation. To ensure an enough operating bandwidth and a small insertion loss of the connector, a V-band Flange Mount Connector (FMC) V103F-R, produced by Anritsu[TM], is chosen in all simulations and measurements. Moreover, the two steps over the ground must be consistent to dimensions of the FMC for the purpose of mounting the connector, and in this design it is set to be a fixed length and thickness, i.e., 16 mm (consistent to the connector) and 2 mm (for considerations of mechanical strength and small influence), respectively, in all simulations and measurements.

Two substrate layers are employed to easily and accurately build an elliptical cavity and a bowtie feeder by the convenient micro-machined PCB technologies in our lab. The feeder are printed on the first layer (top layer), a Rogers 5880 substrate with a thickness of $h_1 = 0.127$ mm (0.005″) and a relative dielectric constant of $\varepsilon_1 = 2.2$ (The first substrate layer is set to be transparent in Fig. 1 to clear show the whole antenna structures), and the elliptical cavity are built on the second one, a Rogers 5870 substrate with a thickness of $h_2 = 1.574$ mm (0.062″) and a relative dielectric constant of $\varepsilon_2 = 2.33$, formed by metalizing the vertical wall of a machined elliptical hole on the substrate. Meanwhile, thickness of the metalized layers on the vertical wall of the cavity is approximately 9 μm, equal to that of the cladding copper layers of both substrates. The elliptical cavity with an major-to-minor axis ratio of R_a and a minor axis (along x axis) of R is centered at the original point of the coordinate system.

Four screws with a 1 mm and around 1.8 mm diameters of lead part and circular nut currently available in our laboratory are considered in simulations and also utilized to build the antenna prototype. Influences of such four "big" screws relative to the operating wavelength on antenna patterns and gains are so obvious that they cannot be neglected in the design procedure, as shown in next part. However, due to confliction with the steps, four screws are not arranged

rotationally symmetric relative to the cavity, but symmetric along x axis. Meanwhile, in order to firmly mount both substrate layers on the ground without damages to them, especially the first layer due to extreme thinness, metal pads under the screws are necessary, and models of these pads must be built in simulations to evaluate their influences.

Figure 1(c) shows details of the first substrate layer. A transition from a 50-Ω microstrip line to a parallel strip line (PSL) (transition I) is connected to the other one from the PSL to a feeding port of a bowtie exciter (transition II), and an output impedance of transition II is designed around 100 Ω for better and easier impedance matching. Design of a 50-Ω microstrip line on the first layer is very easy after the substrate is selected, and additionally one can reference our previous data to design the bowtie exciter [33, 36, 37]. In this design, a rounded sectorial bowtie dipole with a flare angle of 120° is etched on both sides of the first substrate, resulting in flat input impedance around 100 Ω, but even so impedance matching over such a large frequency band is still a significant problem depending on the designs of two transitions. Parameter determinations of two transitions are a little complicated and need careful adjustments, especially the transition II which dominates the impedance matching to a great degree. Most of critical design parameters are labeled in Fig. 1, and a part of their values are directly given in the figure in mm, and the left are given as follows: $R = 3.5$, $R_a = 1.0$, $L_g = 15$, $W_g = 15$, $S_x = 9$, $S_y = 10$, $d_e = 2.5$, $R_p = 2$, and $L = 4.2$.

3. PARAMETRIC STUDIES AND DISCUSSIONS

All simulations in this paper were done by Ansoft High Frequency Structure Simulator (HFSS^{TM}). It should be noted that not all components of the antenna, including the screws, pads, steps and connector, will positively contribute to the antenna radiations, but they are certainly necessary for measurements. Therefore, their influences should be investigated beforehand because they actually bring obvious disturbance on antenna performances due to the electrically large dimensions. Moreover, it is known that different size of these components will also cause different influences, but some of them are in their standard size, e.g., connector and screws, meanwhile the steps are designed in the smallest size to reduce their influence to the lowest level. Thus only the differences of the antennas with and without them are given in Fig. 2 for brevity.

It is clear from Fig. 2(a) that the antenna fed by a real connector will present a smaller operating bandwidth and worse impedance
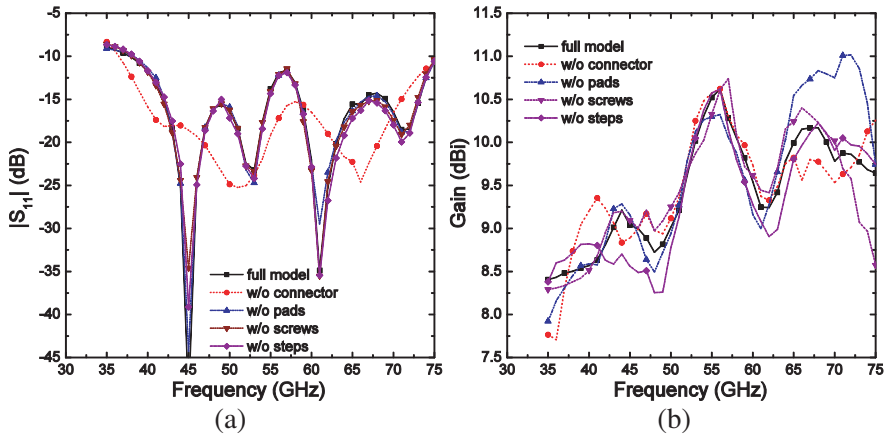
Figure 2. Comparisons of simulated reflection coefficient and gain between the proposed antenna with/without considering the influences of connector, pads, screws and steps, respectively. (a) Reflection coefficient comparison. (b) Gain comparison.

matching than the one without connector (fed by a 50-Ω lumped port in simulations) and the other components bring very slight effects on impedance matching because of a larger distance from the antenna cavity and the feedline. However from Fig. 2(b), each component will significantly change the antenna broadside gain, which indirectly shows that the radiation patterns will also be changed. Firstly because of the electrically large size, the induced currents on the connector surfaces will reshape the H-plane radiation patterns of the antenna, especially those on the surface close to the inverted L-shaped ground, causing gain variations over almost the whole operating band. Actually, influence of the steps is also in a similar manner to the connector, i.e., disturbing the H-plane radiation patterns by the induced currents on their surfaces. Secondly, four pads with a diameter of $R_p = 2\,\text{mm}$ act as four shorted patches with the help of the screws (their height is equal to $h_1 = 0.127\,\text{mm}$), or as four normal circular patches when without the screws, indirectly fed by mutual coupling, so the whole antenna can be considered as a five-element array. Thus the antenna without the pads or the screws shows obviously different gain, especially at higher frequencies. Additionally, due to limitation of mounting, the two pads and screws close to the connector is 1 mm nearer to the cavity than the other ones, causing different strength of influence.

Figure 3 gives the current distributions on the ground of the first substrate layer, the bowtie exciter, and the feedline of the full antenna model at 50, 55, 6, 65 and 75 GHz, which can give further explanations
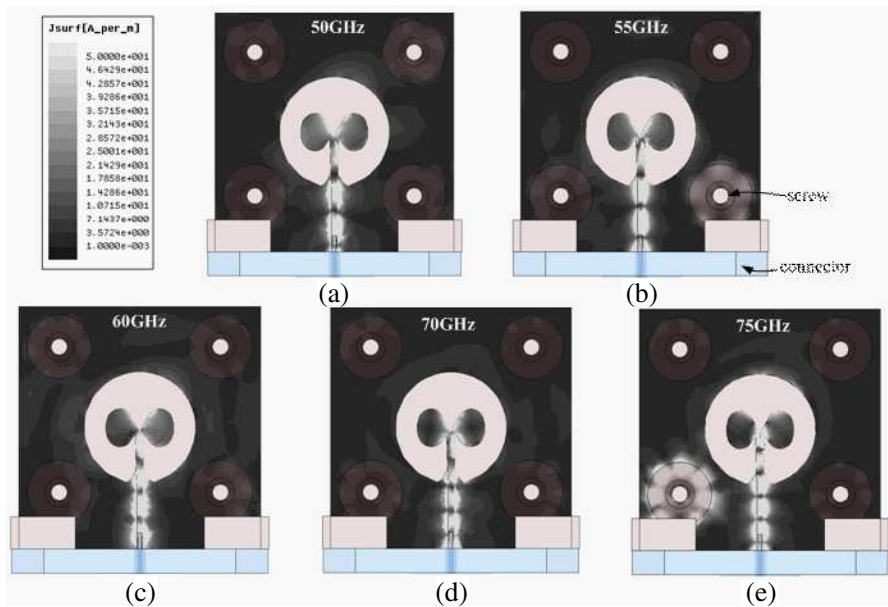
Figure 3. Current distributions on the ground of the first substrate layer, the bowtie exciter, and the feedline of the full antenna model at (a) 50 GHz, (b) 55 GHz, (c) 60 GHz, (d) 65 GHz, and (e) 75 GHz.

on Fig. 2. At 55 and 6 GHz, each antenna model shows a sharp gain augmentation and drop, and 75 GHz is the highest interesting frequency. The current distributions are actually not symmetric due to the antenna asymmetric structure and non-ideally balanced transitions. It can be observed that at 55 GHz the currents on two pads close to the connector is obviously stronger than those at 6 GHz, and these currents give a positive contribution to the antenna gain in a similar manner to a multi-element array. However, the strong currents on the pads at 75 GHz shows more operating modes, and a medium gain is featured after a complex superposition with many modes in the cavity aperture.

From above investigations, it is clear that each component associated to the antenna will obviously change its performance, unlike antennas operating in microwave frequency bands. Therefore, to clearly show how the cavity dominate the antenna performance without interference of the screws, pads, and steps, as shown in Fig. 4(a), they are removed in the parametric studies, meanwhile the real connector model is also replaced by a smaller wave port which is necessary for antenna feeding and proper excitation in simulations.

Figure 4 shows how the major-to-minor axis ratio R_a exerts its influence on antenna reflection coefficient and broadside gain. It can be seen from Fig. 4(b) that as R_a is over 1, it will not obviously change the reflection coefficient except a little offset of resonant frequencies. When R_a is varied from 0.9 to 1.4, i.e., the antenna aperture dimensions along y axis become larger and larger, the antenna can be matched in an acceptable extent and features similar operating bandwidth, because the presented antenna has already been designed to be electrically large for many reasons, e.g., smaller influences of fabrication tolerance (Actually it can operate at lower frequencies as long as suitable impedance matching structure is adopted), and dimensions of the antenna aperture will put more effects on broadside gains, instead of reflection coefficient.

Therefore, it is also easy to understand why the antenna gain becomes larger as R_a increases from 0.9 to 1.4 at lower frequency
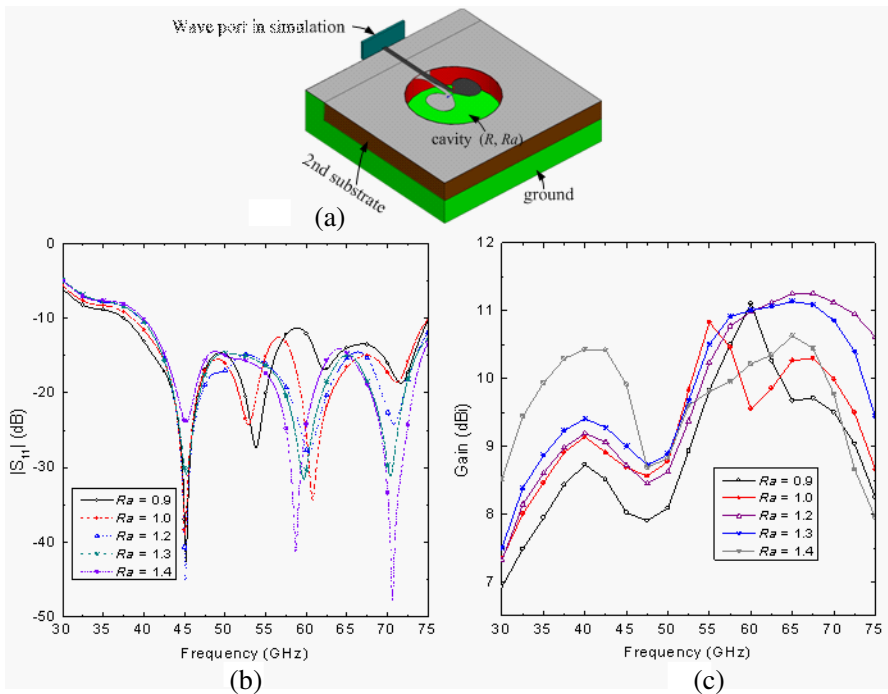

Figure 4. Simulated results of reflection coefficient and gain versus different major-to-minor axis ratio R_a of the cavity. (a) Antenna without screws, pads, and steps. (b) Reflection coefficient versus R_a. (c) Gain versus R_a.
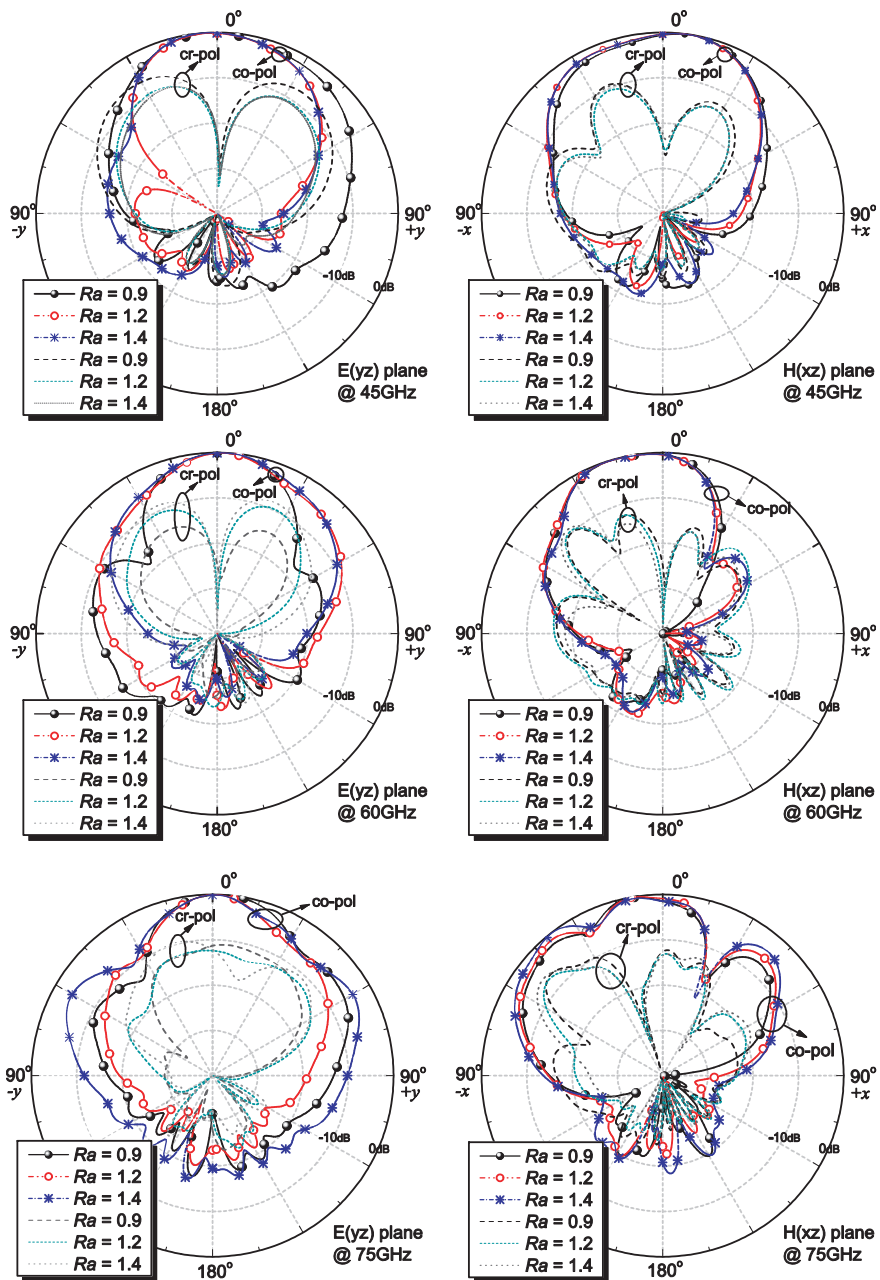
Figure 5. Comparisons of radiation patterns of the proposed antenna versus different major-to-minor axis ratio R_a at 45, 60, and 75 GHz.

band. However, since more and more modes will be excited over the antenna aperture as frequency is beyond 42 GHz, a gain drop, side lobes, and broadening of radiation patterns will occur. Moreover, in higher frequency band, multi-mode dominated radiating behavior becomes clearer, as shown in the comparisons of radiation patterns in Fig. 5. The larger R_a, the broader the radiation patterns and the larger side lobes are, especially at 75 GHz. In contrast, a smaller R_a at lower frequencies, e.g., 45 GHz in Fig. 5, results in a broader E-plane radiation pattern due to relatively smaller aperture size. Additionally, detailed studies on several other parameters of the bowtie exciter can reference our previous works [33, 36, 37].
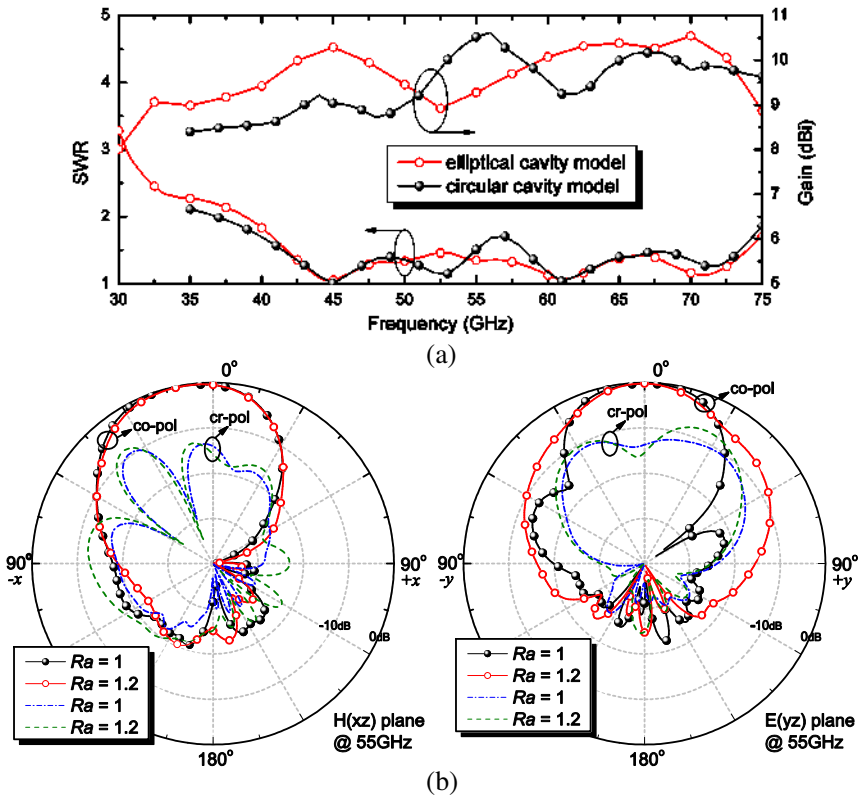

Figure 6. Performance comparisons of the antennas with circular ($R_a = 1$) and elliptical cavities ($R_a = 1.2$) (full model). (a) Comparisons of simulated SWRs and broadside gains. (b) Comparisons of radiation patterns at 55 GHz.

4. EXPERIMENTAL RESULTS

To verify the validity of above simulations, an antenna prototype was fabricated and measured after the parametric studies. Simulations of two full antenna models with $R_a = 1$ and 1.2 are carefully performed, as shown in Fig. 6. It can be seen that the antenna with circular cavity shows slightly larger impedance bandwidth but smaller broadside gain in most of the operating frequency band, because its aperture
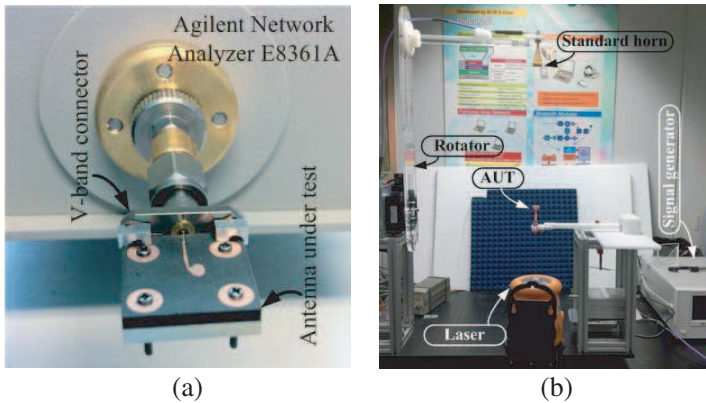

(a)   (b)

Figure 7. Photograph of the fabricated antenna prototype under test. (a) Impedance measurement. (b) Radiation pattern measurement.
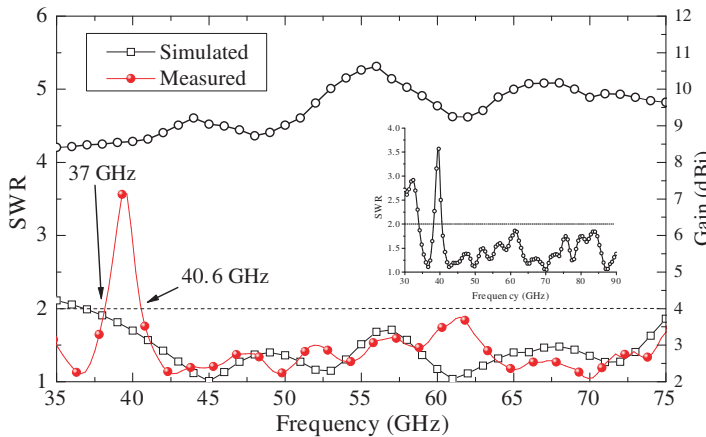

Figure 8. Simulated and measured SWRs and broadside gain of the fabricated antenna prototype.

dimensions are smaller than those of the one with $R_a = 1.2$. However, at around 55 GHz, the former presents a larger gain, and radiation patterns in Fig. 6(b) give the behavior of both antennas at 55 GHz.

Although no obvious differences are found in the H-plane patterns, the E-plane patterns are quite different, and the one with a circular cavity features a thinner pattern than the latter (small side lobes can hardly influence the broadside gain), which means that the multi-mode operation will negatively dominate performances of the former over 55 GHz but has already done below 55 GHz for the latter. Meanwhile, compared with the simulated antenna gains in Fig. 4, the results in Fig. 6 are obviously different, proving significant influences of
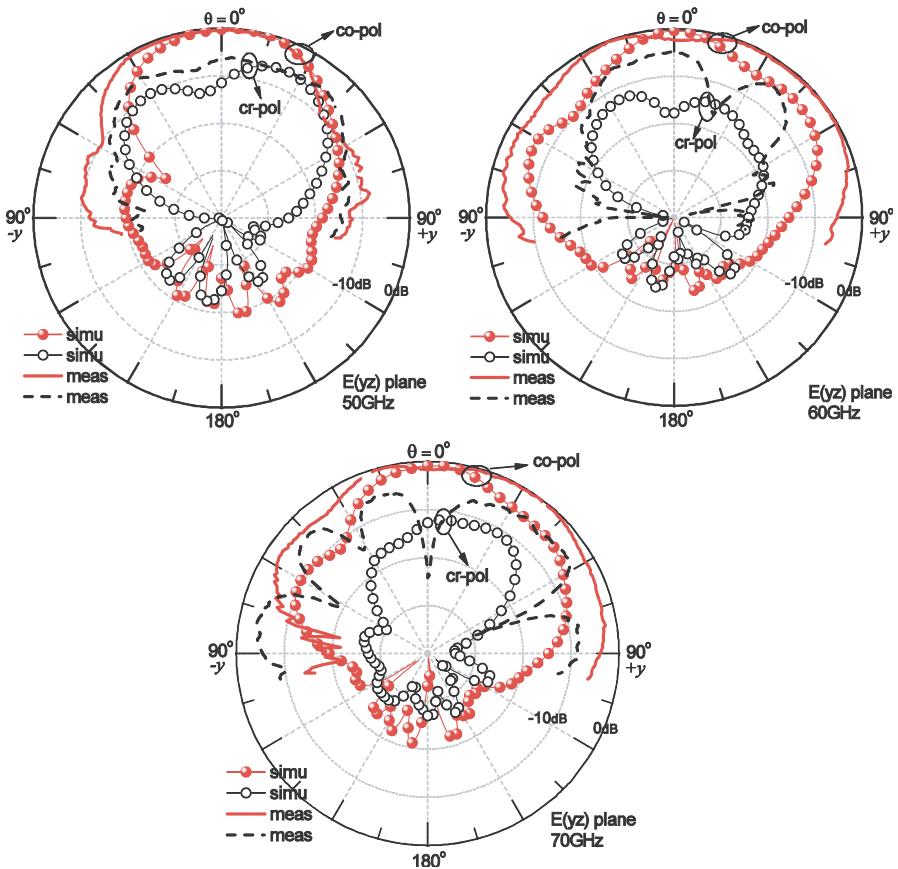

Figure 9. Simulated and measured radiation patterns of the fabricated CBA prototype.

connector, pads, screws and steps again. Finally, the antenna with $R_a = 1$ is chosen for easier fabrications and verification purpose, although the one with $R_a = 1.2$ shows higher broadside gain.

Firstly two substrate layers are fabricated by the LPKF ProtoLaser S laser system structures in our lab and the inverted L-shaped ground are made by conventional machining techniques, then they are assembled along with the Anritsu connector V103F-R into a full antenna prototype by the screws introduced above. The photograph of the prototype is shown in Fig. 7, and its reflection coefficient was measured by Agilent Network Analyzer E8361A also in our lab. Radiation patterns were measured by a house-in measurement system, as shown in Fig. 7(b).

Simulated and measured SWRs as well as simulated broadside gain are given in Fig. 8, and simulations agree reasonably with measurements in the frequency band of $40 \sim 75$ GHz (Measurements were done from 30 to 90 GHz). The measured and simulated impedance bandwidths for SWR ≤ 2 cover two large frequency bands, from 37 to over 75 GHz and from 40.6 to over 90 GHz, respectively. It can be seen that the antenna can actually operate at higher frequencies with SWR ≤ 2 although the V-band connector is specified to work under 65 GHz. Resonance at round 40 GHz is caused by air gap between two substrates introduced in the fabrication process. Meanwhile, the simulated broadside gain is $8.6 \sim 10.6$ dBi in the frequency band of over 40 GHz, with a variation of 2 dBi. Simulated and measured E-plane radiation patterns at 50, 60, and 70 GHz, respectively, are shown in Fig. 9. Measured main beams are broadened compared to simulations, and the discrepancies can be attributed to the fabrication errors and the scattering of the measurement environment.

5. CONCLUSION

In this paper, an mm-wave CBA with a bowtie exciter is investigated in the front part, and influences of all components on antenna broadside gain, reflection coefficient, and radiation patterns are carefully studied. An antenna prototype is also built for verifying the validity of simulations, and measured results are discussed. Moreover, the proposed CBA can also be improved by a composite cavity in antenna radiation patterns and broadside gains. According to our previous investigations [38, 39], the composite cavity can help to obtain flatter gain, more stable radiation patterns, and easier impedance matching etc..

Applications of the proposed CBA can be variant, e.g., highly integrated 60-GHz WLAN systems. As shown in [40], an integrated

circuit (IC) of transceiver can be connected to the antenna by bonding wires, and generally deployed as close as possible to avoid large loss of the mm-wave transmission line. For our proposed CBA, there are two possible ways to integrate them. The first one is to connect the transceiver to the CBA at the feeding microstrip line end, and the other more practical method is to place the transceiver IC at the vertexes of the bowtie exciter for a differential feeding. Meanwhile, the top substrate layer can act as a cover to protect the transceiver.

ACKNOWLEDGMENT

REFERENCES

1. Soliman, E. A., et al., "Series-fed microstrip antenna arrays operating at 26 GHz," *IEEE Int. Symp. Antennas Propagat. Soc.*, 1–4, 2010.

2. Huang, K.-C. and D. J. Edwards, *Millimetre Wave Antennas for Gigabit Wireless Communications*, John Wiley & Sons Ltd., United Kingdom, 2008.

3. Kolak, F. and C. Eswarappa, "A low profile 77 GHz three beam antenna for automotive radar," *IEEE MTT-S Int Microw. Symp. Digest*, Vol. 2, 1107–1110, 2001.

4. Rebollo, A., et al., "A broadband radiometer configuration at 94 GHz in planar technology," *IEEE MTT-S Int. Microw. Workshop Series on Millimeter Wave Integration Technol. (IMWS)*, 89–92, 2011.

5. Schulwitz, L. and A. Mortazawi, "Millimeter-wave dual polarized L-shaped horn antenna for wide-angle phased arrays," *IEEE Trans. on Antennas and Propagat.*, Vol. 54, No. 9, 2663–2668, Sept. 2006.

6. Xu, O., "Diagonal horn gaussian efficiency enhancement by dielectric loading for submillimeter wave application at 150 GHz," *Progress In Electromagnetics Research*, Vol. 114, 177–194, 2011.

7. Miura, Y., et al., "Double-layer full-corporate-feed hollow waveguide slot array antenna in the 60-GHz band," *IEEE Trans. on Antennas and Propagat.*, Vol. 59, No. 8, 2844–2851, Aug. 2011.

8. Bakhtafrooz, A. and A. Borj, "Novel two-layer millimeter-wave

slot array antennas based on substrate integrated waveguides," *Progress In Electromagnetics Research*, Vol. 109, 475–491, 2010.

9. Pan, Y.-M., et al., "Design of the millimeter-wave rectangular dielectric resonator antenna using a higher-order mode," *IEEE Trans. on Antennas and Propagat.*, Vol. 59, No. 8, 2780–2788, Aug. 2011.

10. Perron, A., et al., "High-gain hybrid dielectric resonator antenna for millimeter-wave applications: Design and implementation," *IEEE Trans. on Antennas and Propagat.*, Vol. 57, No. 10, 2882–2992, Oct. 2009.

11. Cui, B., C. Wang, and X.-W. Sun, "Microstrip array double-antenna (MADA) technology applied in millimeter wave compact radar front-end," *Progress In Electromagnetics Research*, Vol. 66, 125–136, 2006.

12. Nesic, A., et al., "Millimeter wave printed antenna array with high side lobe suppression," *IEEE Int. Symp. Antennas Propagat. Soc.*, 3051–3054, 2006.

13. Pozar, D. M., "Considerations for millimeter wave printed antennas," *IEEE Trans. on Antennas and Propagat.*, Vol. 31, No. 5, 740–747, Sept. 1983.

14. Costanzo, S., I. Venneri, G. D. Massa, and G. Amendola, "Hybrid array antenna for broadband millimeter-wave applications," *Progress In Electromagnetics Research*, Vol. 83, 173–183, 2008.

15. Douvalis, V., et al., "A monolithic active conical horn antenna array for millimeter and submillimeter wave applications," *IEEE Trans. on Antennas and Propagat.*, Vol. 54, No. 5, 1393–1398, May 2006.

16. Nguyen, T. K., T. A. Ho, I. Park, and H. Han, "Full-wavelength dipole antenna on a GaAs membrane covered by a frequency selective surface for a terahertz photomixer," *Progress In Electromagnetics Research*, Vol. 131, 441–455, 2012.

17. Matekovits, L., M. Heimlich, and K. P. Esselle, "Metamaterial-based millimeter-wave switchable leaky wave antennas for on-chip implementation in GaAs technology," *Journal of Electromagnetic Waves and Applications*, Vol. 25, No. 1, 49–61, 2011.

18. Yeap, S. B., et al., "Gain-enhanced 60-GHz LTCC antenna array with open air cavities," *IEEE Trans. on Antennas and Propagat.*, Vol. 59, No. 9, 3470–3473, Sept. 2011.

19. De Lange, G., et al., "Development of a 3×3 micromachined millimeter wave SIS imaging array," *IEEE Trans. on Appl. Superconductivity*, Vol. 7, No. 2, 3593–3597, Jun. 1997.

20. Camblor-Diaz, R., S. Ver-Hoeye, C. Vazquez-Antuna, G. R. Ho-topan, M. G. Fernandez, and F. Las-Heras, "Sub-millimeter wave frequency scanning 8×1 antenna array," *Progress In Electromagnetics Research*, Vol. 132, 215–232, 2012.

21. Kramer, O., et al., "Very small footprint 60 GHz stacked Yagi antenna array," *IEEE Trans. on Antennas and Propagat.*, Vol. 59, No. 9, 3204–3210, Sept. 2011.

22. Hayashi, Y., et al., "Millimeter-wave microstrip comb-line antenna using reflection-canceling slit structure," *IEEE Trans. on Antennas and Popagat.*, Vol. 59, No. 2, 398–406, Feb. 2011.

23. Akkermans, J. A. G., et al., "Balanced-fed planar antenna for millimeter-wave transceivers," *IEEE Trans. on Antennas and Propagat.*, Vol. 57, No. 10, 2871–2881, Oct. 2009.

24. Seki, T., et al., "Millimeter-wave high-efficiency multilayer parasitic microstrip antenna array on teflon substrate," *IEEE Trans. on Antennas and Propagat.*, Vol. 53, No. 6, 2101–2106, Jun. 2005.

25. Thakur, J. P., W.-G. Kim, and Y.-H. Kim, "Large aperture low aberration aspheric dielectric lens antenna for W-band quasi-optics," *Progress In Electromagnetics Research*, Vol. 103, 57–65, 2010.

26. Hua, C. Z., X. D. Wu, N. Yang, and W. Wu, "Millimeter-wave homogenous cylindrical lens antenna for multiple fan-beam scanning," *Journal of Electromagnetic Waves and Applications*, Vol. 26, Nos. 14–15, 1922–1929, 2012.

27. Kamchouchi, H. E. and G. Abouelseoud, "A novel approach to multiband- ultra-wideband millimeter wave antennas design based on repeated kernel array of microstrip patches (ReKAMP)," *IEEE Int. Symp. Antennas Propagat. Soc.*, 246–249, 2005.

28. Kumar, A. and H. D. Hristov, *Microwave Cavity Antennas*, Artech House, Norwood, MA, 1989.

29. Li, R., D. Thompson, et al., "Development of a wide-band short backfire antenna excited by an unbalance-fed H-shaped slot," *IEEE Trans. on Antennas and Propagat.*, Vol. 53, No. 2, 662–671, Feb. 2005.

30. Li, R., D. Thompson, et al., "A circularly polarized short backfire antenna excited by an unbalance-fed cross aperture," *IEEE Trans. on Antennas and Propagat.*, Vol. 54, No. 3, 852–859, Mar. 2006.

31. Ou Yang, J., S. Bo, J. Zhang, and F. Yang, "A low-profile unidirectional cavity-backed log-periodic slot antenna," *Progress In Electromagnetics Research*, Vol. 119, 423–433, 2011.

32. Wang, F. J. and J.-S. Zhang, "Wideband cavity-backed patch antenna for PCS/IMT2000/2.4 GHz WLAN," *Progress In Electromagnetics Research*, Vol. 74, 39–46, 2007.

33. Qu, S.-W., "Study on wideband cavity-backed bowtie antennas," Ph.D. Dissertation, The City University of Hong Kong, 2009.

34. Hua, C. Z., X. D. Wu, and W. Wu, "A cavity-backed aperture-coupled microstrip patch antenna array with sum/difference beams," *Journal of Electromagnetic Waves and Applications*, Vol. 26, No. 7, 932–941, 2012.

35. Grzyb, J., et al., "Wideband cavity-backed folded dipole superstrate antenna for 60 GHz applications," *IEEE Int. Symp. Antennas Propagat. Soc.*, 3939–3942, 2006.

36. Qu, S.-W., et al., "Wideband cavity-backed bowtie antenna with pattern improvement," *IEEE Trans. on Antennas and Propagat.*, Vol. 56, No. 12, 3850–3854, Dec. 2008.

37. Qu, S.-W. and C.-L. Ruan, "Effect of round corners on bowtie antennas," *Progress In Electromagnetics Research*, Vol. 57, 179–195, 2006.

38. Qu, S.-W., et al., "Ultrawideband composite cavity- backed folded sectorial bowtie antenna with stable pattern and high gain," *IEEE Trans. on Antennas and Propagat.*, Vol. 57, No. 8, 2478–2483, Aug. 2009.

39. Qu, S.-W., C. H. Chan, and Q. Xue, "Ultrawideband composite cavity-backed rounded triangular bowtie antenna with stable patterns," *Journal of Electromagnetic Waves and Applications*, Vol. 23, Nos. 5–6, 685–695, 2009.

40. Lee, J., et al., "A low-power low-cost fully integrated 60-GHz transceiver system with OOK modulation and on-board antenna assembly," *IEEE J. Solid-State Circuits*, Vol. 45, No. 2, 264–275, Feb. 2010.